GONIOMETER TO MEASURE THE ANGULAR DISTRIBUTION OF NARROW-BAND SOFT X-RAY CHERENKOV RADIATION

W. Knulst*, O.J. Luiten and M.J. van der Wiel, Eindhoven University of Technology, Eindhoven, The Netherlands
J. Verhoeven, FOM-AMOLF, Amsterdam, The Netherlands

Abstract

Cherenkov radiation is a potential narrow-band source based on small accelerators for the soft X-ray region. An experimental set-up has been designed to be able to study the angular intensity distribution of soft X-ray Cherenkov radiation generated by 10 MeV electrons. The accuracy of the set-up will enable investigation of different potential emitters, e.g. C, Ti and V, and also enable a new method of retrieving the optical constants at the absorption edges with a high accuracy.

1 INTRODUCTION

We are investigating Cherenkov radiation as a source for narrow-band radiation in the soft X-ray region. Until now the Cherenkov effect has received little attention among effects to generate soft X-ray radiation by interaction of electrons with a medium, e.g. coherent bremsstrahlung, channing radiation, parametric x rays, and transition radiation. Just recently, we have observed narrow-band silicon L-edge Cherenkov radiation generated by 5 MeV, with a yield of 10^{-3} photon/electron [1]. These measurements show that efficient generation of soft X-ray Cherenkov radiation (XCR) is possible with moderate electron energies.

So far, only XCR at silicon L-edge [1,2] and carbon K-edge [2,3] have been experimentally observed. Theoretical calculations [4] based on the most up-to-date refractive index data [5] have revealed materials that are potential Cherenkov emitters. A few elements, e.g. C, Ti and V, have their XCR emission within the "water window" region (•ω = 284-243 eV), which may be used as a source for x-ray microscopy. Therefore, the upcoming experiments will focus on these materials. In this paper the experimental set-up will be presented in which the XCR intensity and spectrum can be measured as function of emission angle with high angular resolution. These accurate measurements enable a new method to probe the optical constants at absorption edges. The angular dependence of the Cherenkov radiation in relation to the refractive index data will be discussed in section 2. The design of the experimental set-up will be presented in section 3.

2 X-RAY CHERENKOV RADIATION

Cherenkov radiation is emitted by a charged particle if its velocity (v) exceeds the phase velocity of light (c/n) and is therefore limited to the wavelength regions where the real part of the refractive index exceeds unity ($n > 1$). In the soft X-ray region this is only possible in narrow regions of resonant anomalous dispersion at atomic absorption edges.

* w.knulst@tue.nl

2.1 XCR spectral line shape

The XCR spectral output is the result of a very subtle interaction between refraction and absorption of a material, resulting in emission of narrow-band radiation. Material properties are described by a complex dielectric constant: $n(\omega)^2 \equiv \varepsilon(\omega) \equiv 1+\chi'(\omega)+i\chi''(\omega)$, where the real part of the susceptibility, χ', describes the dispersion and the imaginary part, χ'', the absorption. In Fig. 1(a) the complex susceptibility of silicon around the L edge is plotted versus photon energy. In Fig. 1(b) the corresponding XCR spectral yield $dN/d\omega$ is plotted as function of photon energy for 5 MeV electrons passing through a 10 μm foil, which is given by the approximate expression [2]:

$$\frac{dN}{d\omega} = \frac{\alpha}{\omega}\left(\frac{\chi'(\omega)-\gamma^{-2}}{\chi''(\omega)}\right) \qquad (1)$$

with α the fine structure constant and γ the Lorenz factor.

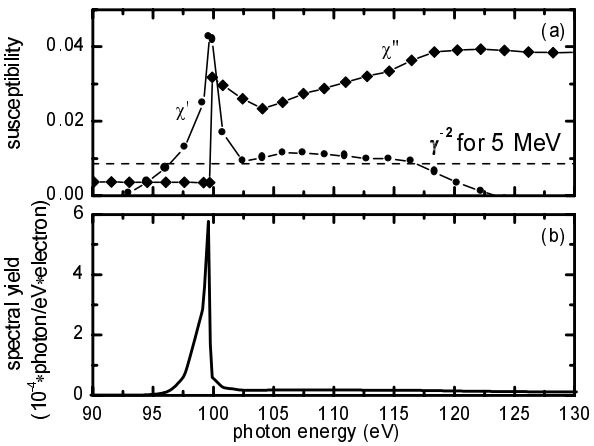

FIG. 1. (a) Real part (χ', circles) and imaginary part (χ'', diamonds) of the susceptibility of silicon as a function of photon energy around the L edge [5]. The Cherenkov threshold for 5 MeV electrons is indicated by a dashed line. (b) Cherenkov spectral yield for 5 MeV electrons in a 10 μm silicon foil. [1]

Since the absorption χ'' is approximately constant in the photon energy region below the absorption edge where the Cherenkov condition ($\chi'>\gamma^{-2}$) holds, the Cherenkov spectral yield as function of photon energy follows the real part of the susceptibility (χ'). The step in χ'' (the

absorption edge) cuts off part of the spectrum generated at higher photon energies, finally resulting in a narrow, asymmetric line in front of the edge.

2.2 XCR angular dependence

Cherenkov radiation can be seen as a 'shockwave of light' that is propagating under the angle of constructive interference. Therefore, XCR is emitted in the forward direction in a cylindrical cone around the electron trajectory. For the soft X-ray region and relativistic electrons, the angular dependence can be approximated by [1]

$$\theta(\omega) = \sqrt{\chi'(\omega) - \gamma^{-2}} \qquad (2)$$

If Eq. (2) is inserted into Eq. (1) then the spectral yield, integrated over the complete solid angle, is proportional to the square of the emission angle. Thus, the XCR photon energy, intensity and emission angle are strongly related.

2.3 Using XCR to probe optical constants

Our previous calculations of Cherenkov radiation for several materials [4] are based on the most up-to-date available database [5]. Nevertheless, the number of data points available in de resonant anomalous region is very limited (see Fig. 1(a)). Moreover, the data points close to absorption edges are subject to large uncertainties [6]. These refractive index values are either based on absorption measurements or on total reflection measurements. In the first case the real part of the refractive index is calculated from the imaginary part by the Kramers-Kronig relation, which is not accurate at absorption edges. In the second case for each photon energy the complex refractive index is fitted to a reflection graph. Direct measurements of the real part of the refractive index are very scarce, because soft X-ray interferometers are very difficult to build [7].

We propose to use XCR as a new probe of the optical constants at absorption edges. The spectral intensity and the emission angle of XCR are very sensitive to the exact values of the refractive index [Eq. 1 and 2]. The real part of the refractive index can be retrieved from the angular spectral measurements by using Eq. 2. Therefore, we have designed a goniometer set-up, which will be able to measure the angular spectral Cherenkov intensity.

The desired accuracy of the goniometer puts constrains on the acceptable electron beam energy spread. The influence of the energy spread on the emission angle is given by:

$$\Delta\theta \approx \frac{1}{\theta(\omega)\gamma^2}\frac{\Delta E}{E} \qquad (3)$$

The angular spread diverges at $\theta=0°$, but the XCR yield is then also zero. The maximum emission angle of the XCR, based on the refractive index data, for 10 MeV electrons is generally above 1°. To achieve 1 mrad angular resolution at angles larger than 1° the energy spread has to be limited to 0.74% for a 10 MeV beam energy.

In Fig. 2 the theoretical relative accuracy of a measurement of the refractive index is plotted as function of detection angle when χ' is calculated from spectral angular measurements by using Eq. 2.

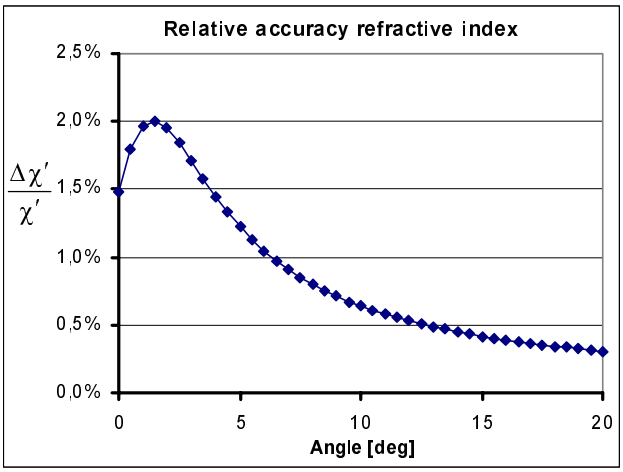

Fig. 2. Relative accuracy of the measurement of χ' based on Eq. (2) plotted for 1 mrad angular spread and 0.74% energy spread.

3 EXPERIMENTAL SET-UP

The electron source of the experimental set-up is a 10 MeV travelling wave linear accelerator (LINAC). This is a standard medical LINAC, which can operate from 9 to 11 MeV depending on the macro pulse current. This LINAC generates an electron beam with a typical energy spread of 3.5% and a transverse (un-normalized) emittance of about 10 π mm mrad.

The desired angular accuracy of 1 mrad is realized in the goniometer design by the combination of 1 mm beam size and 1 meter detector distance. For this reason the (un-normalized) transverse beam emittance on the target foil has to be 1 π mm mrad in the vertical plane (see paragraph 3.2). To match the electron beam to the goniometer, a beam line has been built between the LINAC and the goniometer.

3.1 Beam line between LINAC and goniometer

The energy-spread reduction is realized by closing a slit in the focus point of a bending magnet (see Fig. 3). But by introducing this bending magnet into the beam line the electron beam will suffer from dispersion. To compensate the dispersion, the energy-selecting bending magnet is the first of four bending magnets in a double achromatic bending system. This configuration enables a parallel-to-parallel beam transfer with the ability of energy-spread reduction, if the distance between the bending magnets is equal to $L=\rho/\sin(\theta)$ [8], with ρ the radius and θ the angle of the bending magnet.

To control the emittance of the electron beam at the target position in the goniometer, quadripoles are built into the beam line (see Fig. 3). The triplet $Q_1Q_2Q_3$ matches the electron beam from the LINAC to the bending section. The quadripole Q_4 causes focussing in the plane perpendicular to the bending plane. Finally, the doublet Q_5Q_6 gives the desired emittance at the target position.

There are two dipoles integrated into the doublet to be able to correct for misalignment in the bending section.

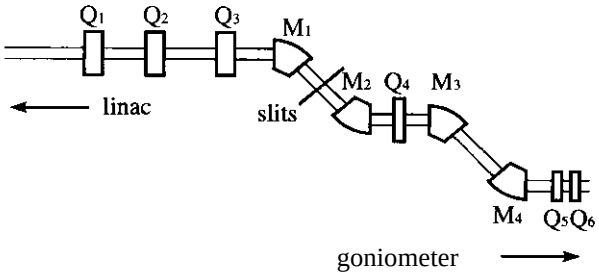

Fig. 3. Detailed layout of the beam line between the LINAC and the goniometer.

The quadripoles are not able to reduce the (preserved quantity) emittance. At the target position the (un-normalized) emittance has to be 1 π mm mrad, but only in the vertical plane (see paragraph 3.2). Therefore, we have introduced directly behind the LINAC a vertical slit, to be able to reduce the phase-space area.

3.2 Goniometer

The angular measurement of the goniometer is restricted to only the vertical plane, because the XCR is cylindrically symmetric. The angular range is set from -20° to +20°, because all the theoretically predicted XCR emitters are within this range.

The target foil holder in the goniometer will be able to turn the foil from perpendicular to parallel position with respect to the electron trajectory. By changing the angle of incidence, the influence on the angular output intensity can be studied. Hopefully, our new accurate measurements will contribute to the discussion in literature [3] about the enhancement of the intensity output at grazing incidence.

3.3 XCR CCD-camera

A CCD-camera specially designed for the soft X-ray region by SRON [9] has been bought. The camera has a back-illuminated CCD-chip (768x1024 pixels) with very high quantum efficiency, which allows single photon counting. By using the photon counting mode a spectrum of the incident radiation can be obtained. The spectral range covers photon energies from 0.250 keV to 15 keV with a quantum efficiency larger than 80%. Typically, the resolution of the CCD-camera is 90 eV at 277 eV and 160 eV at 2.0 keV.

5 CONCLUDING REMARKS

At this moment the presented experimental set-up is under construction. The goniometer will be used to measure the angular distribution of narrow-band XCR generated by 10 MeV electrons in foils of different materials. Additionally, the high angular resolution of the goniometer in combination with the emittance and energy-spread reduction enables 1 mrad accuracy of the measurement. These measurements enable a detailed study of optical constant of materials around the absorption edge. This is a new method of measuring the refractive index of bulk material.

6 REFERENCES

[1] W. Knulst, O.J. Luiten, M.J. van der Wiel and J. Verhoeven, Appl. Phys. Lett. 79, 2999 (2001)

[2] V.A. Bazylev, V.I. Glebov, E.I. Denisov, N.K. Zhevago, and A.S. Khlebnikov, Sov. Phys. JETP Lett. 54, 884 (1981).

[3] M.J. Moran, B. Chang, M.B. Schneider, and X.K. Maruyama, Nucl. Instrum. Methods Phys. Res. B 48, 287 (1990)

[4] W. Knulst, O.J. Luiten, M.J. van der Wiel, and J. Verhoeven, Proc. of the EPAC 2000, 2609 (2000)

[5] B.L. Henke, E.M. Gullikson, and J.C. Davis, At. Data Nucl. Data Tables **54**, 181 (1993), http://www-cxro.lbl.gov

[6] R. Soufli and E.M. Gullikson, Appl. Opt. **36**, 5499 (1997)

[7] D. Joyeux, F. Polack, D. Philippou, Rev. Sci. Instr. **70**, 292 (1999)

[8] R.W. de Leeuw, J.I.M. Botman, I.F. van Maanen, C.J. Timmermans, G.A. Webers, and H.L. Hagedoorn, Proc. of the 1994 EPAC, 2417 (1994)

[9] J.W. den Herder, *et al.*, Astron. Astrophys. **365**, L7 (2001)